

**TRANSITIONAL AND TURBULENT FLOW
DRIVEN BY A ROTATING MAGNETIC FIELD
IN A CYLINDRICAL CONTAINER**

K. Frana, J. Stiller, R. Grundmann

*Institute for Aerospace Engineering (ILR), Dresden University of Technology,
D-01062 Dresden, Germany (frana@mw.tfd.tu-dresden.de)*

Introduction. We investigate the flow of an electrically fluid driven by a rotating magnetic field (RMF) in a finite-length cylindrical container. Stirring by the RMF plays an important role in applications such as single crystal growth or in metallurgical processes. From a practical point of view, the effect of the RMF on the conductive fluid is characterized by the generation of a primary swirling flow (Moffatt [1]). Furthermore, in the case of a closed container, Bödewadt-type layers are created at the axial boundaries which, in turn, drive a weak meridional flow. Several authors, e.g., Priede & Gelfgat [2], Kaiser & Benz [3], Mössner & Gerbeth [4] carried out axisymmetric simulations of the laminar and near-critical flow regimes. However, Grants & Gerbeth [5] found that the first linearly unstable mode is three-dimensional in a wide range of aspect ratios. This implies that any numerical study of supercritical flow requires a three-dimensional approach. The aim of this work is to present a first insight in the 3D structures and dynamics of the flow in the near-critical and weakly turbulent regimes by means of direct numerical simulation (DNS). The underlying mathematical model rests upon on the so-called low-frequency/low-induction approximation, which is appropriate for stirring of liquid metals and semiconductor melts.

Mathematical model. We consider a fluid with constant properties, i.e., density ρ , kinematic viscosity ν and electric conductivity σ . The computational domain is a closed cylinder of height H , diameter $D = 2R$ and non-conducting walls. The magnetic field of induction B rotates with a constant angular velocity ω about the axis. The resulting flow is governed by the Naviers-Stokes equations,

$$\begin{aligned} \partial_t \mathbf{u} + \nabla \cdot \mathbf{u}\mathbf{u} &= -\frac{1}{\rho} \nabla p + \nu \nabla^2 \mathbf{u} + \frac{1}{\rho} \mathbf{f}, \\ \nabla \cdot \mathbf{u} &= 0. \end{aligned} \quad (1)$$

Under low-frequency/low-induction conditions (Davidson & Hunt [6]) the Taylor number (2) is the only relevant parameter:

$$\text{Ta} = \frac{\sigma \omega B^2 R^4}{2\rho\nu^2}. \quad (2)$$

Furthermore, the mean part of the Lorentz forces is independent on the velocity field and is defined in Eq. 3 (Gorbachev, Nikitin & Ustinov [9]):

$$\mathbf{f}(z, r) = \frac{1}{2} \sigma \Omega B^2 \left[r - R \sum_{k=1}^{\infty} \frac{2J_1(\lambda_k r/R) \cosh(\lambda_k z/R)}{(\lambda_k^2 - 1) J_1(\lambda_k) \cosh(\lambda_k H/2R)} \right] \mathbf{e}_\varphi. \quad (3)$$

Here J_1 is the Bessel function of the first kind and λ_k are the roots of its first derivatives. The equations are discretized in space using the pressure-stabilized

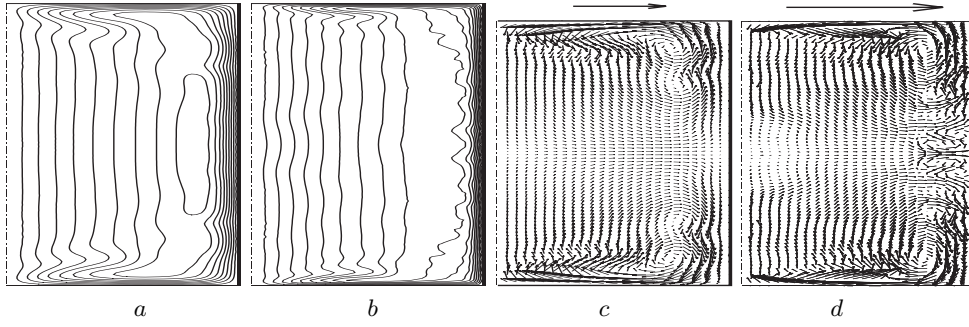


Fig. 1. Mean velocity field: (a), (b) \bar{u}_φ at $Ta = 4.5 \cdot 10^4$ and $Ta = 3 \cdot 10^5$; (c), (d) (\bar{u}_r, \bar{u}_z) at $Ta = 4.5 \cdot 10^4$ and $Ta = 3 \cdot 10^5$.

Petrov–Galerkin finite element method (PSPG-FEM) and integrated in time by means of the 2nd order Adams–Bashforth method. The numerical model was implemented on top of MG (multilevel grid) package (Stiller & Nagel [7]). The validation for several test cases proved the second-order convergence in time and space (Stiller *et al.* [8]).

Results. DNS were carried out at various Taylor numbers ranging from 1.1 to $7.5 Ta_{cr}$, where $Ta_{cr} = 40079$ (G.Gerbeth, private communication [5]). In the following, we focus on $Ta = 4.5 \cdot 10^4$ and $Ta = 3 \cdot 10^5$. For the case with the Taylor number $4.5 \cdot 10^4$ the computational grid consists of $7.1 \cdot 10^6$ tetrahedral elements or $1.3 \cdot 10^6$ nodes. However, for $Ta = 3 \cdot 10^5$ the grid was locally refined to resolve the thin Bödewadt type boundary layers developing at the top and bottom walls. The resulting grid consists of $9.7 \cdot 10^6$ elements and $1.8 \cdot 10^6$ nodes, respectively.

Fig. 1 shows the mean velocity field at $Ta = 4.5 \cdot 10^4$ and $Ta = 3 \cdot 10^5$. In the averaging process the axial and vertical symmetries were exploited. Fig. 1a and 1b demonstrate the existence of a widely homogeneous swirling flow. The meridional flow is depicted in Fig. 1c and 1d. Near the top and bottom, the formation of Bödewadt layers is evident. Except of the wall layers, the meridional flow gets weaker with increasing Taylor numbers. Fig. 2 shows a snapshot of the instantaneous velocity field in a meridional section. The primary flow is homogeneous in the core region, but becomes more irregular near the vertical walls (see Fig. 2a and 2b). This fact can be attributed to the action of Taylor–Görtler type vortices. The existence of those vortices is confirmed by Fig. 2c and 2d which depict the meridional velocity components.

The Taylor–Görtler vortices have an important impact on the instantaneous velocity distribution. To visualize the vortex structures, the second invariant of the fluctuation velocity gradient was used (Fig. 3). Obviously, the TG vortices

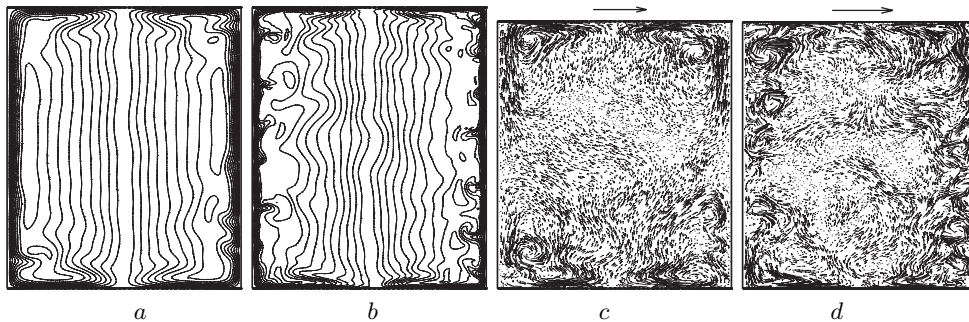


Fig. 2. Snapshot of the instantaneous velocity field in the meridional section: (a), (b) u_φ at $Ta = 4.5 \cdot 10^4$ and $Ta = 3 \cdot 10^5$, (c), (d) (u_r, u_z) at $Ta = 4.5 \cdot 10^4$ and $Ta = 3 \cdot 10^5$.

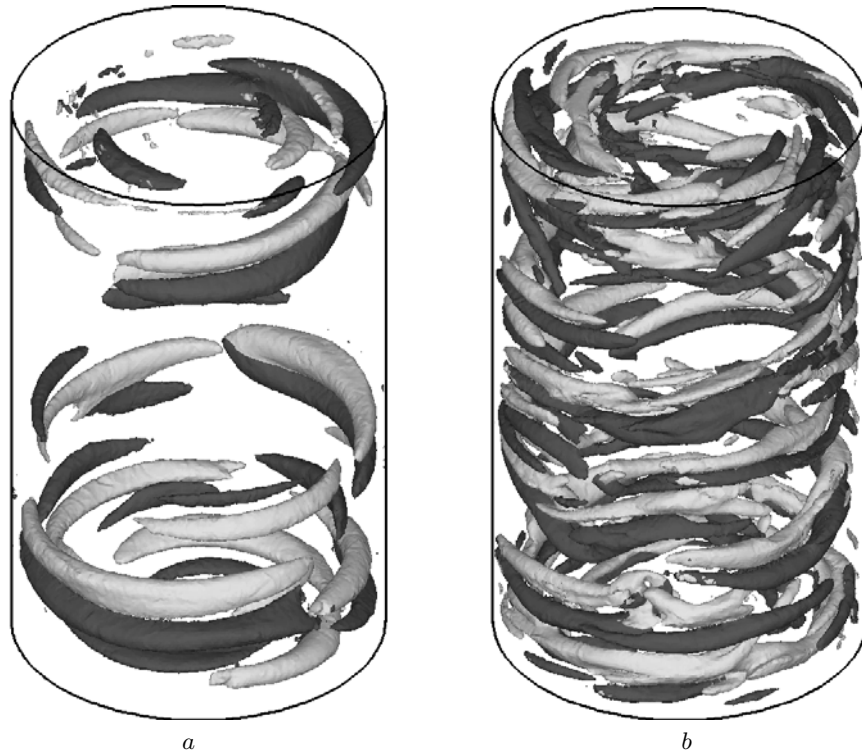


Fig. 3. Taylor–Görtler type vortices at the Taylor numbers $4.5 \cdot 10^4$ and $3 \cdot 10^5$.

become more slender and unstable with the increasing Taylor number. In particular at $Ta = 3 \cdot 10^5$, bifurcation, merging as well as tearing and reconnection of vortices can be observed. Finally, Fig. 4 shows a typical energy spectrum at $Ta = 3 \cdot 10^5$. Evidently, no harmonic oscillations can be observed. In the first part of the inertial range, the slope is close to the classical $k^{-5/3}$ decay, later the slope

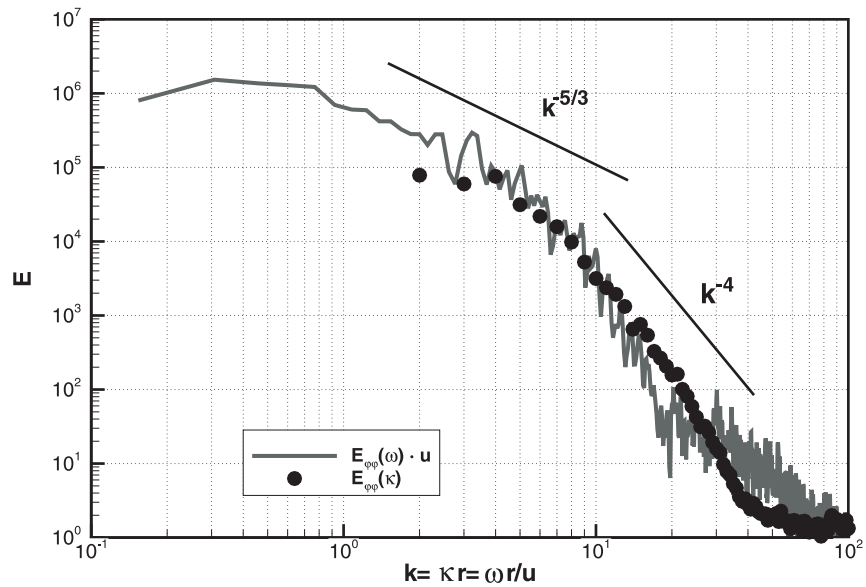


Fig. 4. Energy spectrum at the Taylor number $3 \cdot 10^5$.

is considerably steeper. Recent results by Cramer & Varshney (private communication) suggest that a similar behaviour can be found also in experimental data. A further discussion of these observations will be the subject of the future work.

Conclusion. The RMF driven flow at the near-critical Taylor numbers was investigated by means of DNS. For all cases, the flow was characterized by a primary azimuthal flow and a weak secondary meridional flow. In agreement with Grants & Gerbeth [5], the flow of the near-critical Taylor number is unsteady and three-dimensional. The existence of Taylor–Görtler vortices and their impact on the instantaneous flow field was demonstrated.

Acknowledgments. Financial support from German "Deutsche Forschungsgemeinschaft" in the frame of the Collaborative Research Center SFB 609 is gratefully acknowledged.

REFERENCES

1. H.K. MOFFATT. On fluid flow induced by a rotating magnetic field. *J. Fluid Mech.*, vol. 22 (1965), pp. 521–528
2. J. PRIEDE, YU.M. GELFGAT. Numerical simulation of the MHD flow produced by a rotating magnetic field in a cylindrical cavity in finite length. *Magnetohydrodynamics*, vol. 33 (1997), pp. 172–179.
3. TH. KAISER, K.W. BENZ. Taylor vortex instabilities induced by a rotating magnetic field: A numerical approach. *Physics of Fluids*, vol. 10 (1998), no. 5, pp. 1104–1109.
4. R. MÖSSNER, G. GERBETH. Buoyant melt flows under the influence of steady and rotating magnetic fields. *Journal of Crystal Growth*, vol. 197 (1999), pp. 341–354.
5. I. GRANTS, G. GERBETH. Linear three-dimensional instability of a magnetically driven rotating flow. *J. Fluid Mech.*, vol. 463 (2002), pp. 229–239.
6. P.A. DAVIDSON, J. HUNT. Swirling recirculation flow in a liquid-metal column generated by a rotating magnetic field. *J. Fluid Mech.*, vol. 18 (1987), pp. 67–106.
7. J. STILLER, W.E. NAGEL. MG - A Toolbox for Parallel Grid Adaption and Implementing Unstructured Multigrid Solver In *E.H.D'Hollander et al.*, ((Eds.): Parallel Computing matrices and vectors,2001), pp. 391–399.
8. J. STILLER, K. FRANA, R. GRUNDMANN, U. FLADRICH, W.E. NAGEL. A parallel PSPG Finite Element Method for direct Simulation of Incompressible flow. *Euro-Par 2004, Parallel Processing, 2004*.
9. L.P. GORBACHEV, N.V. NIKITIN, A.L. USTINOV. Magnetohydrodynamic rotation of an electrically conductive liquid in a cylindrical vessel of finite dimension. *Magnetohydrodynamics*, vol. 10 (1974), pp. 406–414.